Theoretical Investigation of Arene Alkylation by Ethene and Propene over Acidic Zeolites

Bjørnar Arstad,[†] Stein Kolboe,*[,†] and Ole Swang[‡]

Department of Chemistry, University of Oslo, P.O. Box 1033 Blindern, N-0315 Oslo, Norway, and SINTEF Applied Chemistry, Department of Hydrocarbon Process Chemistry, P.O. Box 124 Blindern, N-0314 Oslo, Norway

Received: May 30, 2003; In Final Form: October 21, 2003

Arene alkylation with ethene or propene over acidic zeolites has been investigated by quantum chemical calculations using a simplified zeolite model; a four T-atom cluster. Four different arenes are alkylated in this work: benzene, toluene, 1,3,5-trimethylbenzene, and pentamethylbenzene. The species resulting from toluene alkylation have been restricted to the para-isomers. Alkylation with propene formed *n*-propyl- and isopropylarenes. All the studied reactions are concerted reaction types with no intermediates between the alkene protonation step and ethyl/propyl-group formation on the arene. The reactions proceed by a simultaneous transfer of a proton from the cluster to the alkene, and formation of a C−C bond between the alkene and the arene. Dealkylations are also discussed, as elimination of alkyl groups from alkylarenes plays a central role in the methanol-to-hydrocarbons reaction. Comparisons between calculated and experimental values are done where possible. Computed energy trends are in good agreement with reported experimental data. The influence of different reactants on activation energies, reaction energies, and reaction paths is discussed.

1. Introduction

Ethylbenzene and isopropylbenzene (cumene) have important industrial applications. Combined, these two chemicals account for nearly 75% of the world's consumption of petrochemical grade benzene.[1] The compounds are both used mainly as intermediates in the chemical industry: Cumene as a raw material for phenol and acetone, and ethylbenzene in the production of styrene by dehydrogenation. The two compounds were traditionally obtained industrially by a Friedel−Crafts alkylation using $AlCl_3$ as catalyst. Zeolite-type catalysts now mostly replace the aluminum halide, as they offer environmental and economical advantages. Typical catalysts are based on H−ZSM-5, MCM-22, dealuminated mordenite, and H−Beta.

1-Ethyl-4-methylbenzene (*p*-ethyltoluene) is dehydrogenated to *p*-methylstyrene, which may be polymerized to yield poly(*p*-methylstyrene) that has certain advantages over polystyrene. Formation of *p*-ethyltoluene over acidic zeolites has been the subject of several experimental studies.[2−4] High purity fractions of *p*-isopropyltoluene (*p*-cymene) are used in the production of fungicides, pesticides, flavors, and perfumes and as a heat transfer medium, etc.[5] Its synthesis is preferably carried out over acidic zeolites, and a high para-selectivity can be obtained with zeolites of MFI structures.[6,7] Synthesis of mono- and dialkylbenzenes over zeolite catalysts was recently reviewed by Cejka et al.[8]

The original motivation for the present work comes from our earlier studies on the methanol-to-hydrocarbons (MTH) process.[9−15] A now increasingly accepted reaction mechanism (the hydrocarbon pool mechanism) is based on experiments showing that arenes, and especially methylbenzenes, are important intermediates in the MTH mechanism in SAPO-34, H−ZSM-5, and other zeotype materials.[12−18] A methyl−arene hydrocarbon pool mechanism includes repeated methylations of the arenes by methanol, forming multiply substituted methylbenzenes, and, at a later step, rearrangement to higher alkylbenzenes. The products, typically ethene and propene, are then split off, forming a less alkylated benzene that may again be methylated, thus closing the catalytic cycle. The mechanistic details of alkene formation from alkylbenzenes are, however, still unclear. By study of arene alkylation as done here, information may also be obtained on the reverse process, dealkylation. Both directions of the reactions studied in the present work are of interest because dealkylation is the last step in the MTH hydrocarbon pool mechanism.

In a preceding work,[15] we described the mechanism for methylation of toluene, durene, and hexamethylbenzene by methanol. A mechanism for the formation of higher alkyl groups in a polymethylbenzene has been proposed by Sassi et al.[18] In the present work, the rearrangements leading to higher alkyl groups on the benzene ring are not discussed. We discuss briefly a possible elimination route for alkene formation from an alkylarene, particularly ethyl- or (iso)propylbenzene.

Experimental studies of reactions within the confining walls of microporous materials are challenging, and quantum chemical studies may be a useful complement to experimental work. In the present work, we investigate the direct (as opposed to a two-step process where the alkene first forms an alkoxide on the zeolite wall and is subsequently transferred to the arene) alkylation of the four arenes benzene, toluene, 1,3,5-trimethylbenzene (1,3,5-triMB), and pentamethylbenzene (pentaMB) with ethene and propene using density functional theory (DFT) and ab initio methods. The acidic site in the zeolite material is represented by a cluster model containing four T-atoms, one of which is aluminum. Toluene alkylation has been restricted to alkylation in the para-position only. This gives twelve reactions in all, as propene may give two isomers for each arene. The products formed in these 12 reactions are: ethylbenzene, *p*-ethyltoluene, 1-ethyl-2,4,6-trimethylbenzene (1-ethyl-2,4,6-

* To whom correspondence should be addressed.
[†] University of Oslo.
[‡] SINTEF Applied Chemistry.

10.1021/jp0307147 CCC: $27.50
Published on Web 01/28/2004

triMB), ethylpentamethylbenzene (ethylpentaMB), propylbenzene, *p*-propyltoluene, 1-propyl-2,4,6-trimethylbenzene (propyl-2,4,6-triMB), propylpentamethylbenzene (propylpentaMB), isopropylbenzene, *p*-isopropyltoluene, 1-isopropyl-2,4,6-trimethylbenzene (isopropyl-2,4,6-triMB), and isopropylpentamethylbenzene (isopropylpentaMB).

Very recently, Vos et al. have reported the formation of ethylbenzene and isopropylbenzene with similar calculation techniques as used in the present work.[19] Comparison with that work is made when relevant.

2. Computational Details

All calculations were carried out with the Gaussian 98 program package.[20] All geometry optimizations were performed without imposing any geometry constraints using the B3LYP hybrid density functional with 6-31G* basis sets. The integration grid for the DFT calculations was set to "ultrafine". Additionally, single-point energies were calculated with the B3LYP/6-311G**, B3LYP/cc-pVTZ, and MP2/6-311G** schemes for the geometries thus obtained. The zeotype material has been modeled by a cluster containing four T-atoms, as detailed earlier.[15] Care has been taken to ensure that reactants and products coordinate similarly to the cluster for all reactions. This makes comparisons for trends easier but should otherwise not influence the results, because there are no constraints. It is conceivable that it might be possible to find a stationary state where one adsorbed molecule located on the "back side" of the cluster. This would correspond to a position inside the zeolite framework, outside the pore system, so it would no more mimic a reaction taking place in a zeolite. Such a position has been avoided.

For all stationary states, vibrational spectra were calculated to ensure that there was the correct number of imaginary frequencies. Zero for the minima and one for the transition states. The transition states were investigated further by perturbing their geometries very slightly along the reaction coordinate corresponding to the negative eigenvalue in the Hessian, and using the geometries resulting from this perturbation as starting points for energy minimizations. In each case, these tests confirmed that the transition states connected the desired energy minima. Zero point energies have been calculated for all the stationary points at the B3LYP/6-31G* level of theory. In the following, B3LYP/6-31G* energies with zero point corrections will be used if not stated otherwise. Our conclusions are, however, independent of the choice of method.

3. Results

3.1. Adsorbed Reactants. Figure 1 gives a schematic view of the adsorbed reactants. Table 1 gives important interatomic distances and angles using geometric labels, as defined in Figure 1. Table 2 gives the adsorption energies. We have chosen to investigate the reaction where the alkene is adsorbed on the acidic proton on the zeolite. The alkene π-electrons are directed toward the acidic proton. For all optimized coadsorbed reactants, the alkene is adsorbed on the acidic site. The arene is adsorbed edge-on. The proton may then attack the alkene, which may then perform an electrophilic attack on the arene. Figures 2 and 3 convey a visual impression. Corma et al.[21] concluded from their experimental measurements that propene, and not benzene, is likely to be adsorbed on the acidic site in the cumene formation reaction on MCM-22. Their findings support our choice of having the alkene adsorbed on the acidic site and the arene coadsorbed beside the alkene in the starting structures of the studied reactions.

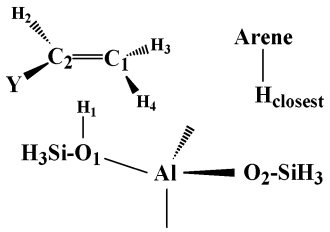

Figure 1. Schematic presentation of the most important geometric characteristics for the adsorbed reactants. Y is a CH_3 group when propene is adsorbed. $H_{closest}$ is an H-atom on the aromatic ring except for adsorbed pentamethylbenzene where it is on a methyl group.

TABLE 1: Most Important Geometric Characteristics of the Adsorbed Reactants[a] (Distances in Ångstroms, Angles in Degrees)

	ethene + benzene	ethene + toluene	ethene + 1,3,5-triMB	ethene + pentaMB
O_1H_1	0.99	0.99	0.99	0.99
C_1H_1	2.26	2.26	2.30	2.28
C_2H_1	2.26	2.26	2.28	2.28
C_1C_2	1.34	1.34	1.34	1.34
$H_{closest}O_2$	2.74	2.74	2.72	2.77[b]
C_1O_1	3.22	3.22	3.26	3.24
C_2O_1	3.21	3.21	3.21	3.21
$C_1C_2H_1O_1$	175	175	161	164
	propene + benzene	**propene + toluene**	**propene + 1,3,5-triMB**	**propene + pentaMB**
O_1H_1	0.99	0.99	0.99	0.99
C_1H_1	2.16	2.16	2.20	2.19
C_2H_1	2.31	2.31	2.27	2.27
C_1C_2	1.34	1.34	1.34	1.34
$H_{closest}O_2$	2.69	2.69	2.75	2.75[b]
C_1O_1	3.13	3.13	3.17	3.16
C_2O_1	3.24	3.24	3.19	3.18
$C_1C_2H_1O_1$	173	173	162	163

[a] $H_{closest}$ is the H-atom on the arene, which is closest to an O-atom on the zeolite. $H_{closest}$ is on the aromatic ring except when pentamethylbenzene is the adsorbed arene, then $H_{closest}$ is on a methyl group. See Figure 1 for atomic label definitions. [b] $H_{closest}$ is on a methyl group.

As can be seen from Table 1, there are no substantial differences in the geometric parameters describing the adsorption whether the alkene is ethene or propene, or with a changing number of methyl groups on the arene. When ethene is adsorbed, the two C−H distances C_1H_1 and C_2H_1 are all but identical. In the unsymmetrical propene molecule, C_1H_1 is considerably shortened, and C_2H_1 is correspondingly lengthened relative to ethene. The asymmetry is in full accord with general chemical knowledge that when an alkene is protonated, the proton attaches to the least substituted carbon. No clear-cut effect on the C−H distances of replacing one arene by another is observed. The O_1H_1 distance is independent of the coadsorbed arene. Adsorbed ethene and propene do not change their double bond lengths when different arenes are coadsorbed.

The arene H-atom that is closest to the cluster, an O-atom, is ca. 2.7 Å away. This is in agreement with the empirically known van der Waals radii of the two atoms. This H-atom is part of a methyl group when pentaMB is the coadsorbed arene; in other cases it is directly bonded to the aromatic ring.

The adsorption energies given in Table 2 show that the DFT results are quite similar in all cases (31−36 kJ/mol), and the MP2 adsorption energies are almost twice these values (ca. 59−78 kJ/mol). The presently available density functionals are known to describe dispersion energies (London forces) poorly. The exchange-correlation potential $V_{xc}(r)$ at a given point r is

TABLE 2: Adsorption Energies (kJ/mol) of the Reactants Relative to the Gas Phase Reactants

adsorbed species on the zeolite model	adsorption energy				
	B3LYP/ 6-31G*+ZPE	B3LYP/ 6-31G*	B3LYP/ 6-311G**	B3LYP/ cc-pVTZ	MP2/ 6-311G**
ethene + benzene	−33	−39	−26	−24	−59
ethene + toluene	−33	−39	−27	−24	−60
ethene + 1,3,5-triMB	−31	−38	−25	−21	−66
ethene + pentaMB	−31	−36	−27	−20	−67
propene + benzene	−36	−41	−29	−27	−67
propene + toluene	−36	−41	−30	−27	−68
propene + 1,3,5-triMB	−35	−41	−28	−24	−75
propene + pentaMB	−35	−39	−22	−24	−78

determined by the density (and its gradients) at this point. This means that the energy at a given point is unaffected by another distant system if there is no electron density overlap.[22] In the present work, the MP2 values are the more realistic adsorption energies. The whole set of atomic positions in the adsorbate system is given as Supporting Information.

The adsorption energies found by Vos et al. (absolute values) are slightly lower compared to the ones given in Table 2.[19] They reported E_{ads}(ethene+benzene) = −30.5 kJ/mol, whereas we found −32.6 kJ/mol. Further, they reported E_{ads}-(propene+benzene) = −34.5 kJ/mol, where our value is −36.0 kJ/mol. The energy differences might be caused by slightly different geometries of the adsorbed state, and in addition, Vos et al. report some small imaginary frequencies for their

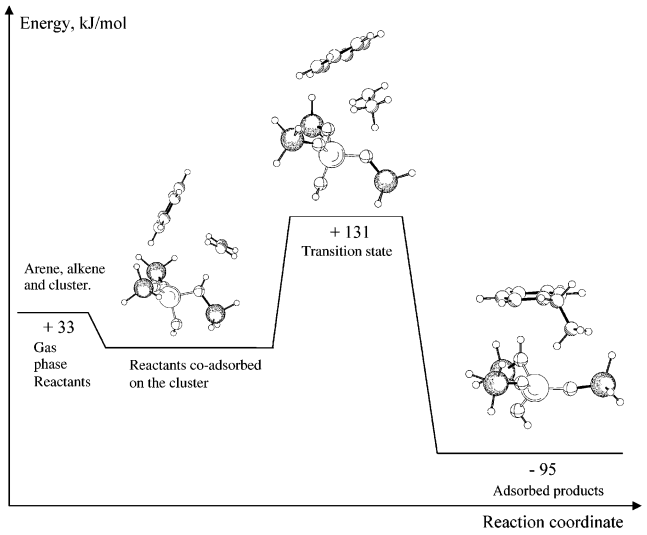

Figure 2. Reaction energy diagram of the ethylation of benzene on a cluster. B3LYP/6-31G* + ZPE corrected energies.

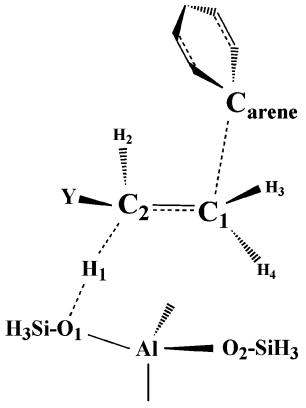

Figure 3. Schematic presentation of the most important geometric characteristics in the ethylation and *n*-propylation transition states. Y is a CH_3 group when propene is the alkylating reagent.

TABLE 3: Most Important Geometric Characteristics for the Arene Ethylation Transition States[a] (Distances in Ångstroms, Angles in Degrees)

	ethyl-benzene TS	*p*-ethyl-toluene TS	1-ethyl-2,4,6-triMB TS	ethyl-pentaMB TS
O_1H_1	1.71	1.63	1.52	1.50
C_2H_1	1.17	1.19	1.23	1.23
C_2H_2	1.10	1.10	1.09	1.09
C_2C_1	1.42	1.42	1.41	1.41
C_2Y[b]	1.09	1.09	1.09	1.09
C_1C_{arene}	2.39	2.43	2.45	2.42
C_1Al	3.63	3.68	3.69	3.72
C_1H_3	1.09	1.09	1.09	1.09
C_1H	1.09	1.09	1.09	1.09
HO_2	2.01	2.08	2.21	2.20
C_2O_1	2.82	2.78	2.71	2.72
$C_{arene}C_1C_2$	114	113	114	114
$H_1C_2C_1$	97	97	97	97
$O_1H_1C_2$	156	160	163	167
$C_{arene}C_1C_2H_1$	159	162	160	169
$C_1C_2H_1O_1$	−71	−79	−92	−94
$H_4C_1C_2H_3$	−155	−156	−156	−154
Im freq	157i	207i	369i	367i

[a] See Figure 3 for atomic label definitions. [b] Y is an H-atom.

computed minima. The nonbonding C_1H_1 distances are longer in their case (0.02 Å), for both alkenes, than we found. The distances between bonded atoms appear identical, however.

3.2. Ethylation Reactions. Alkylations of benzene, toluene, 1,3,5-trimethylbenzene, and pentamethylbenzene by ethene give ethylbenzene, 1-ethyl-4-methylbenzene, 1-ethyl-2,4,6-trimethylbenzene, and 1-ethyl-2,3,4,5,6-pentamethylbenzene as products. A reaction energy diagram for the ethylation of benzene is given in Figure 2, and a schematic representation of the catalyzed ethylation of arenes is given in Figure 3. For simplicity, hydrogen or methyl groups on the arene are not shown. The dashed lines indicate bonds that are broken or formed during the reaction. They also give an indication of the normal mode the transition state reaction coordinate moves along. In the transition state, the proton H_1 attacks an ethene carbon atom, C_2, and simultaneously, the other ethene carbon, C_1, starts forming a bond with an arene carbon, C_{arene}. By comparing the data in Tables 1 and 3, and taking benzene ethylation as an example, while keeping in mind Figures 2 and 3, one can see clear differences. In the transition state O_1H_1 is markedly lengthened, from 0.98 to 1.71 Å. C_2H_1 becomes much smaller; it changes from 2.26 to 1.17 Å. C_1C_2 increases from the typical double bond length 1.34 to 1.42 Å, and C_1C_{arene} changes from the noninteracting distance 4.1 to 2.39 Å. This distance is much too long to talk about a C−C bond, but it is much shorter than a van der Waals distance of about 3.5 Å, so there is a nonnegligible interaction.

The features observed for benzene ethylation are to a large extent preserved when benzene is replaced by one of the other arenes, but some systematic variations can be seen. Table 3 shows that O_1H_1 decreases with an increasing number of methyl

TABLE 4: Stationary Point Energies (kJ/mol) Relative to the Adsorbed Reactants for the Computational Schemes Used in This Work

	transition state energy					product energy				
products from alkene + arene + H-Zeo	B3LYP 6-31G*+ZPE	B3LYP 6-31G*	B3LYP 6-311G**	B3LYP cc-pVTZ	MP2 6-311G**	B3LYP 6-31G*+ZPE	B3LYP 6-31G*	B3LYP 6-311G**	B3LYP cc-pVTZ	MP2 6-311G**
ethylbenzene	131	135	153	155	160	−95	−106	−89	−87	−127
p-ethyltoluene	123	128	145	147	153	−94	−105	−90	−86	−125
1-ethyl-2,4,6-triMB	109	117	129	132	137	−82	−95	−84	−78	−123
ethylpentaMB	105	113	127	127	135	−64	−77	−62	−59	−113
propylbenzene	147	151	169	172	173	−77	−88	−75	−69	−110
p-propyltoluene	139	143	161	163	166	−76	−87	−73	−69	−109
1-propyl-2,4,6-triMB	127	133	148	149	151	−63	−76	−65	−60	−106
propylpentaMB	123	131	137	146	149	−46	−58	−52	−41	−95
isopropylbenzene	131	129	154	156	145	−76	−86	−70	−67	−118
p-isopropyltoluene	108	112	129	132	134	−76	−86	−69	−66	−118
1-isopropyl-2,4,6-triMB	98	101	114	117	120	−44	−58	−40	−40	−101
isopropylpentaMB	93	98	104	114	124	−23	−36	−27	−17	−83

groups on the arene. Correspondingly, the C_2H_1 distance increases. Overlay of the transition state geometries suggests that the decreasing distance when going from tri- to pentaMB may be a steric effect. The extra methyl group appears to tilt the benzene ring slightly and thereby force the arene carbon nearer C_1. The angles $C_{arene}C_1C_2$ and $H_1C_1C_2$ are the same for all arenes. The angle $O_1H_1C_2$ increases from 156° to 167° showing that the proton moves somewhat closer to the connecting line between O_1 and C_2. The dihedral angle $C_{arene}C_1C_2H_1$ does not change much and shows that the alkyl group addition takes place nearly anti-periplanarly. Table 4 shows that for all computational schemes there is a clear trend for decreasing activation energies when more methyl groups are added to the arene. The ZPE corrected B3LYP/6-31G* energy falls from 131 to 105 kJ/mol when we go from benzene ethylation to pentaMB ethylation. In accordance with the Hammond principle the geometry of the transition state tends to be reached somewhat earlier. The trends, which are seen, are in excellent accord with the known increase in basicity when more methyl groups are added to the benzene ring. The whole set of atomic positions in the transition state systems are given as supplementary information.

The activation barrier for ethylation of benzene reported by Vos et al. is very close to the one found in this work (132 vs 131 kJ/mol).[19] The real difference in transition state energy is, however, somewhat larger. When the "apparent activation energy" ($E_{act} + E_{ads}$) is calculated, Vos et al. obtain 101.4 kJ/mol, whereas in our case the result is 98.4 kJ/mol.

In the benzene ethylation transition state found by Vos et al., the acidic proton is completely attached to the ethene molecule (C−H length is 1.09 Å) and the distance between the acidic proton and the nearest O-atom on the zeolite is 3.69 Å. In the present work the corresponding distances are 1.17 and 1.71 Å. We have found a longer C_1C_{arene} distance than found by Vos et al., 2.39 vs 2.12 Å. The interatomic distances indicate that the benzene ethylation transition state found in the present work is reached at an earlier point along the reaction coordinate than the one found by Vos et al. Even if the two transition states have different geometries, they describe the same reaction and they have similar barrier energies. Not surprisingly, this indicates that several possible reaction paths with very similar barrier heights may lead to the same product. It is with these similar energies impossible to decide which is the preferred one. However, our transition state, besides having a lower energy, describes an anti-periplanar elimination/addition reaction and is chemically more intuitive for concerted alkylation reactions, as described here.

3.3. *n*-Propylation Reactions. It is well-known that when an alkene is protonated (adding a cation) the proton tends to attach to the least substituted double bond carbon. In accordance with this, alkylation of benzene with propene yields mainly isopropylbenzene. Besides a higher barrier, there is, however, nothing to prohibit the proton from adding to the more substituted carbon in the double bond. In that case *n*-propylarene is the expected product. We have investigated both reaction types. *n*-Propyl substitution will be treated first.

The *n*-propylarene transition states are qualitatively similar to the ethylation reactions. The products formed from *n*-propylation of benzene, toluene, 1,3,5-trimethylbenzene, and pentamethylbenzene are propylbenzene, 1-propyl-4-methylbenzene, 1-propyl-2,4,6-trimethylbenzene, and 1-propyl-2,3,4,5,6-pentamethylbenzene. Figure 3 also serves for conveying a schematic view of the *n*-propylation transition states, when Y is taken to represent a methyl group. Figure 4 shows a reaction energy diagram of the *n*-propylation of benzene. Table 5 gives characteristic transition state parameters.

The reaction behavior is very much the same as found previously for the ethylation reaction. In the transition state, the proton, H_1, is leaving the zeolite and is attaching to the middle carbon atom in propene, C_2, initiating formation of a formally primary propyl cation. Simultaneously, C_1 and C_{arene} are closing in for making a C−C bond. As above, propylation of benzene is discussed first, and we concentrate on a

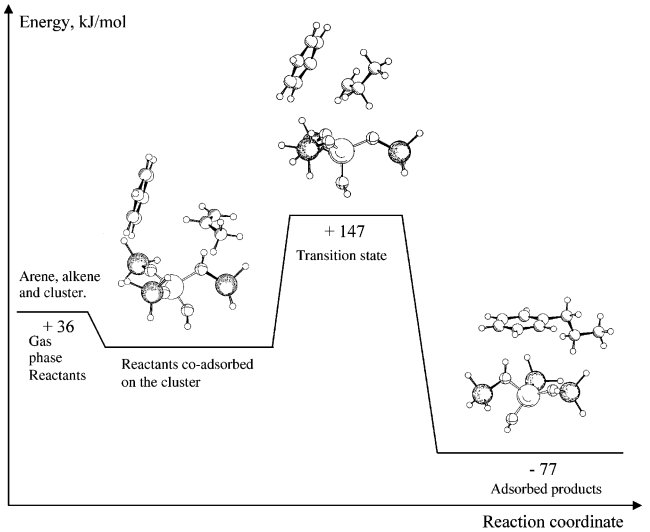

Figure 4. Reaction energy diagram of the *n*-propylation of benzene on a cluster. B3LYP/6-31G* + ZPE corrected energies.

TABLE 5: Most Important Geometric Characteristics for the Arene *n*-Propylation Transition States[a] (Distances in Ångstroms, Angles in Degrees)

	propyl-benzene TS	*p*-propyl-toluene TS	1-propyl-2,4,6-triMB TS	propyl-pentaMB TS
O_1H_1	1.81	1.73	1.62	1.59
C_2H_1	1.16	1.17	1.20	1.21
C_2H_2	1.10	1.10	1.10	1.10
C_2C_1	1.43	1.43	1.42	1.41
C_2Y^b	1.52	1.52	1.52	1.52
C_1C_{arene}	2.33	2.37	2.42	2.43
C_1Al	3.61	3.66	3.66	3.65
C_1H_3	1.09	1.09	1.09	1.09
C_1H_4	1.09	1.09	1.09	1.09
H_4O_2	2.01	2.05	2.19	2.18
C_2O_1	2.90	2.86	2.79	2.77
$C_{arene}C_1C_2$	116	115	116	117
$H_1C_2C_1$	94	94	94	93
$O_1H_1C_2$	155	159	163	164
$C_{arene}C_1C_2H_1$	154	157	157	160
$C_1C_2H_1O_1$	−67	−75	−99	−101
$H_4C_1C_2H_3$	−153	−153	−154	−154
Im freq	122i	147i	224i	239i

[a] See Figure 3 for atomic label definitions. [b] Y is a CH_3-group. The distance is measured to the C-atom.

comparison with the ethylation case. H_1 is further removed from the cluster oxygen; it has moved from 1.71 to 1.81 Å. The C_2H_1 distance has decreased from 1.17 to 1.16 Å. The C_2C_1 bond is slightly longer, being extended to 1.43 Å rather than 1.42 Å in the ethylation case. The C_1C_{arene} distance is considerably shorter. It has fallen from 2.39 to 2.33 Å. All this shows a reaction coordinate that has progressed further toward the product than found above. In agreement with this result, Table 4 shows that the activation energy is considerably higher for *n*-propylation than for ethylation.

Further reference to Table 5 shows that essentially the same trend in interatomic distances as previously found for ethylation is found when more heavily methylated arenes are reacting. The O_1H_1 distance becomes shorter, C_2H_1 becomes longer, the C_2C_1 bond is shortened, and the C_1C_{arene} distance is increased. The reaction coordinate has progressed less toward the product when the transition state is reached. These observations are again in agreement with a marked fall in activation energy, as shown in Table 4. The transition state energies are typically about 15 kJ/mol higher than the corresponding values when ethene is reacting.

The activation energy differences in the alkylation reactions closely follow the exothermicities of the reactions. The reaction energies are typically 18 kJ/mol less exothermic in the *n*-propylation reactions, and this difference correlates well with the increase in activation energies for the *n*-propylations of arenes.

As anticipated, gas phase optimizations to a local minimum on a primary propyl cation failed, as all attempts converged to the secondary cation.

3.4. Isopropylation Reactions. Isopropylation of the arenes result in the formation of isopropylbenzene (cumene), *p*-isopropyltoluene, 1-isopropyl-2,4,6-trimethylbenzene, and isopropylpentamethylbenzene.

Experimentally, it is known that when propene alkylates an arene, isopropyl group formation takes place. Figure 5 shows a reaction energy diagram of the isopropylation of benzene, and Figure 6 gives a schematic view of the transition state in such a case. The figure is very similar to Figure 3, but as the dashed lines show, the reaction follows a different path. Interatomic distances and angles are given in Table 6.

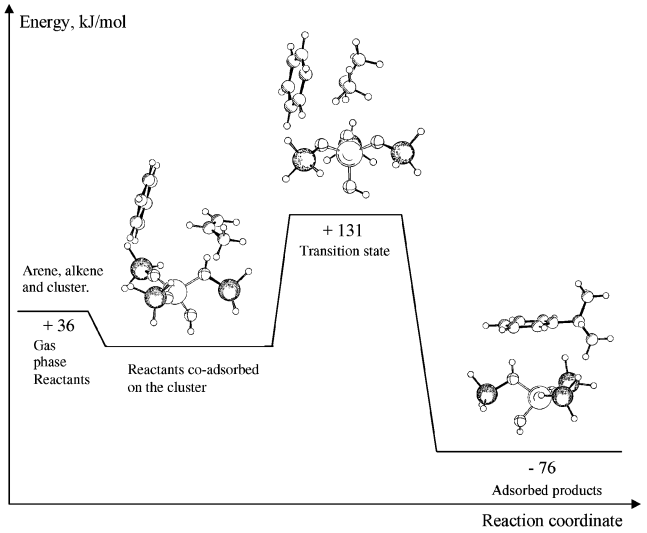

Figure 5. Reaction energy diagram of the isopropylation of benzene on a cluster. B3LYP/6-31G* + ZPE corrected energies.

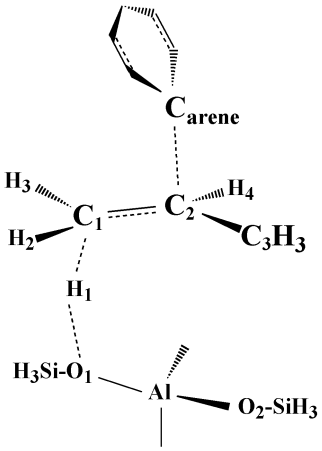

Figure 6. Schematic presentation of the most important geometric characteristics in the isopropylation transition states.

TABLE 6: Most Important Geometric Characteristics for the Arene Isopropylation Transition States[a] (Distances in Ångstroms, Angles in Degrees)

	isopropyl-benzene TS	*p*-isopropyl-toluene TS	1-isopropyl-2,4,6-triMB TS	isopropyl-pentaMB TS
O_1H_1	2.44	2.00	1.92	1.82
C_1H_1	1.10	1.12	1.13	1.14
C_1H_2	1.09	1.09	1.09	1.09
C_1H_3	1.09	1.10	1.09	1.09
C_1C_2	1.49	1.45	1.45	1.44
C_2H_4	1.09	1.10	1.09	1.08
C_2C_{arene}	2.12	2.52	2.50	2.63
C_2C_3	1.50	1.48	1.48	1.48
C_2Al	3.78	3.66	3.58	3.56
C_1O_1	3.23	3.02	3.02	2.95
$C_{arene}C_2C_1$	102	107	107	106
$H_1C_1C_2$	105	101	102	102
$O_1H_1C_1$	127	148	164	170
$C_3C_2C_1H_4$	−141	−157	−154	−160
$C_{arene}C_2C_1H_1$	164	144	153	158
$C_2C_1H_1O_1$	−83	−39	−41	−35
Im freq	151i	26i	38i	17i

[a] See Figure 6 for atomic label definitions.

In the transition state, the proton, H_1, is leaving the zeolite model and is attaching to the end carbon atom in propene, C_1, thereby initiating formation of a formally secondary propyl cation. Simultaneously, C_2 and C_{arene} are closing in for making

a C−C bond. As above, isopropylation of benzene is discussed first, and we concentrate on a comparison with the *n*-propylation case. H_1 is further removed from the cluster oxygen; it has moved from 1.81 to 2.44 Å. Whereas previously the proton moved toward C_2, it has now moved toward C_1. The C−H distance C_1H_1 is reduced compared to the distance, C_2H_1, found for *n*-propylation, 1.10 vs 1.16 Å. The C_1C_2 bond is slightly longer compared to the *n*-propylation reactions, 1.49 vs 1.43 Å. In the adsorbed state before starting the reaction it was (Table 1) 1.34 Å. The gas phase secondary propyl cation, calculated at the same level of theory, has been calculated to be symmetrical with a C_1C_2 distance 1.45 Å. Not surprisingly, the alkylation transition state is not symmetric, and C_2C_3 is 1.50 Å. The difference in length between C_1C_2 and C_2C_3 is admittedly very small, but as Table 5 shows, the nonsymmetry is accentuated in the other cases.

In the *n*-propylation case, the C−C bond formation took place between C_1 and C_{arene}. In the isopropylation case the bond forms between C_2 and C_{arene}. Previously C_1C_{arene} was 2.33 Å; in the present case the corresponding distance, C_2C_{arene}, is 2.12 Å, a marked decrease. The dihedral angle $C_3C_2C_1H_4$ is −141°, in accord with a beginning bond formation between C_2 and C_{arene}. The originally planar structure is transforming into a pyramidal one, with C_2 rising above the other three atoms, and getting closer to C_{arene}. The dihedral angle $C_{arene}C_2C_1H_1$, which is 164°, shows that the reaction is approximately antiperiplanar.

As was found in the other alkylation cases, discussed above, going from a less methylated to a more methylated arene introduces geometric changes, but the differences are small—possibly without chemical significance. It may be mentioned that in the case of benzene isopropylation the arene molecule is located somewhat differently relative to the cluster compared to the other isopropylation transition states. The O_1H_1 distance becomes smaller, but the distance between these atoms is so large in the transition state that there is hardly any interaction between them. The C_1H_1 distance gets longer with increasing number of methyl groups on the arene. The distance is, however, so small that an almost complete proton transfer is apparent. The double bond distance, C_1C_2, is slightly influenced by replacing the arene. It becomes shorter with increasing arene size. The C_2C_{arene} distance shows an increasing trend when we go from benzene to the more methylated arenes, the distances being 2.12, 2.52, 2.50, and 2.63 Å for 0, 1, 3, and 5 methyl groups, respectively.

The benzene alkylation activation energy (Table 4) is seen to be significantly smaller when an isopropylation takes place than when the reaction results in *n*-propylation and is similar or smaller compared to the ethylation of benzene. This result is independent of the calculation scheme used. As found above for ethylation and *n*-propylation, the activation energy decreases markedly when methyl groups are added to the arene. The decrease is, however, small when we go from 1,3,5-triMB to pentaMB.

The activation barrier for isopropylation of benzene reported by Vos et al. is slightly lower than found in this work (124 kJ/mol vs 131 kJ/mol).[19] When the "apparent activation energy" ($E_{act} + E_{ads}$) is calculated, Vos et al. obtained 90 kJ/mol. In our case the result is 95 kJ/mol. The geometries of the transition states are different and this is probably the reason for the different isopropylation energies in the two works.

In both cases, however, the atomic distances concerned with bond breaking or formation are rather similar. The acidic proton is almost completely attached to the propene molecule (C−H bond length in both cases 1.10 Å), and the O−H distance is so long that the remaining interaction is small: 2.80 Å in the paper by Vos et al., and 2.44 Å in our work. We have found a shorter C_2C_{arene} distance than found by Vos et al., 2.12 vs their value 2.28 Å.

The two transition states have different geometries and there is a 5 kJ/mol difference in "apparent" activation energy, indicating that several possible reaction paths may lead to the same product. The relatively small difference in "apparent activation energy" in the two works suggests that the reaction may take place along both paths found in these works. However, our transition state describes a nearly anti-periplanar elimination/addition reaction and is chemically more intuitive for concerted alkylation reactions as described here.

4. Discussion

4.1. Alkylation Reaction. Table 4 shows that alkylation by ethene and propene becomes easier with an increasing number of methyl groups on the arene. The activation energy is markedly lowered, and the lowering is essentially independent of the method used. As an example, isopropylation of pentaMB has a transition state energy about 38 kJ/mol lower than isopropylation of benzene.

The decrease in activation energies is accompanied by increasing bond lengths for the forming C−C bonds in the transition states. The interaction between the two C-atoms, which are to form a bond in the products, will depend on the electron density on the two atoms. The methyl groups on the aromatic ring increase the electron density on the ring C-atoms compared to the electron density in benzene. The higher electron density on these C-atoms makes the molecule more polarizable, and this may be the intuitive reason for lowered activation energy. Reaction energies, on the other hand, become less exothermic with increasing number of methyl groups on the aromatic ring. This falling trend is more pronounced for isopropyl group formation than for *n*-propyl group formation; intuitively, this is to be expected because the isopropyl group is the more bulky.

The computations predict arene ethylations to have lower activation barriers than the corresponding *n*-propylation reactions. This result is again independent of the method used. By comparing the adsorption energies in Table 2 with the corresponding activation energies in Table 4, it is observed that replacing ethene with propene results in a stronger adsorption. The difference in adsorption energy accounts for about half the difference in activation energy. A large fraction of the remaining 5−10 kJ/mol difference might be due to the longer distance from the cluster proton to C_2 (the carbon to be protonated) in propene than to either of C_1 or C_2 in ethene, as seen from Table 1.

In accord with conventional chemical wisdom, transition state energies for isopropylations are lower than the corresponding *n*-propylations. In commercial processes, the amount of *n*-propylbenzene is typically 200−300 ppm in the product mixture.[1] The difference in activation energies of about 16 kJ/mol between the two propylation reactions is in fair accordance with the industrially observed product distribution, provided the process is kinetically controlled. When a propylation reaction is carried out in a zeolite system with fairly narrow pores (H−ZSM-5) there may be a substantial formation of the *n*-propyl isomer. Wichterlova et al.[23] studied toluene propylation in various zeolite systems and concluded that, though important amounts of *n*-propyltoluene could be formed over H−ZSM-5, it was likely to be the result of secondary transalkylation reactions within the zeolite framework. Sponer et al.[24] later

TABLE 7: Reaction Gas Phase Energies and Enthalpies (kJ/mol) for Formation of the Ethyl/Propylarenes Studied in the Present Work[a]

products formed from alkene + arene	calcd gas phase reacn enthalpies B3LYP/ 6-31G*	B3LYP/ 6-311G**	B3LYP/ cc-pVTZ	MP2/ 6-311G**	exp gas phase enthalpies[b]	G3(MP2) reacn enthalpies[c]
ethylbenzene	−104	−85	−82	−124	−106	−105
p-ethyltoluene	−104	−85	−81	−124	−106	−104
1-ethyl-2,4,6-triMB	−91	−73	−66	−120		
ethylpentaMB	−72	−60	−51	−107		−85
propylbenzene	−88	−73	−67	−114	−96	−93
p-propyltoluene	−88	−73	−66	−114		−92
1-propyl-2,4,6-triMB	−74	−58	−52	−111		−88
propylpentaMB	−51	−38	−29	−91		
isopropylbenzene	−87	−70	−64	−122	−99	−97
p-isopropyltoluene	−86	−69	−62	−121		−97
1-isopropyl-2,4,6-triMB	−54	−37	−29	−100		
isopropylpentaMB	−33	−17	−7	−83		

[a] Enthalpies are given at 298 K. The geometries and enthalpy corrections are calculated at the B3LYP/6-31G* level of theory. [b] Reference 32, NIST Chemistry Webbook. [c] Reference 29.

studied the transalkylation reaction by quantum chemical methods and found the data to support the notion that transalkylation is the main route for *n*-propylarene formation.

On the basis of their experimental results, Corma et al. concluded that the cumene formation from propene and benzene proceeds by an Eley-Rideal type mechanism, with an apparent activation energy of 75 kJ/mol.[21] The discrepancy of this value with our calculated energies is hardly surprising and may be attributed to three important effects of the cluster approximation. First, an artificially high proton affinity of the deprotonated cluster, compared to a real zeolite, contributes to increased transition state energies. A lower proton affinity, closer to that found in a real zeolite, would give lower transition state energies.[25] Second, lack of a full electrostatic field is also likely to contribute to higher transition state energies compared to a real zeolite. The electric field within the zeolite will stabilize charged transition states relative to neutral reactants and products.[26] Third, the adsorption energies for reactants, transition states, and products in cluster calculations are too small and are more equivalent to the interaction energy between the reactant and catalytic site.

From periodic DFT calculations on methylation and isomerization reactions of benzene and toluene, Rozanska et al.[27] concluded that cluster models gave qualitatively correct methylation reaction mechanisms and that the cluster model also conserves the relative order of activation energies. However, the transition state energies are higher than they would be in a true zeolite framework. Even if the comparative studies done by Rozanska et al. did not concern alkylation reactions by ethene and propene as done here, the transition states involve in all cases charged species. It therefore seems safe to assume that the reaction barriers found in this work, though being too high, are fair estimates of the relative experimental transition state energies.

To evaluate in more detail the quality of the methods used in the present work, the gas phase reaction energies have also been calculated, and they are given in Table 7. They are compared with reaction enthalpies computed at the B3LYP/6-31G* level of theory, and experimental gas phase reaction enthalpies where available, and G3(MP2) values are taken from Arstad et al.[29] Reaction enthalpies calculated at the B3LYP/6-31G* level of theory give surprisingly good values compared to the experimental and G3(MP2) values. This must, however, be assigned to a fortuitous cancellation of errors. This is shown by single point energies calculated with different basis sets for the reactions in study. By apparently improving the basis sets (using larger basis sets), the reaction energies become less exothermic and deviate more from experiments. Compared to reaction energies over the cluster, the gas phase reaction energies are somewhat more exothermic.

TABLE 8: Gas Phase Reaction Energies (kJ/mol) for Ethylbenzene Formation from Benzene and Ethene with Various Basis Sets and Methods

method	basis set 6-31G*	6-311G**	cc-pVDZ	cc-pVTZ	aug-cc-pVTZ
B3LYP	−116	−97	−107	−94	−92
MP2	−137	−136	−136	−132	−134

Test calculations on the formation of ethylbenzene from benzene and ethene with different basis set were done to shed further light on the energy trends. See Table 8 for a summary of the basis set effect on the reaction energies for ethylbenzene formation. By improving the already large basis set cc-pVTZ with diffuse functions, the B3LYP/aug-cc-pVTZ//B3LYP/6-31G* reaction energy becomes even less exothermic, −92 kJ/mol.

Using a smaller basis set for the single point energy, the B3LYP/cc-pVDZ//B3LYP/6-31G* scheme, makes the reaction energy more exothermic compared to the cc-pVTZ basis set, −107 kJ/mol. These results point in the direction that the larger basis sets are stabilizing the reactants more in some way relative to the products. A larger basis set might describe more properly the correlation energies in the reactant fragments compared to the products. During the reaction, the alkene double bond ($1\pi + 1\sigma$) is transformed into two σ-bonds, those of the alkyl group on the arene. One might speculate that correlation effects are more important for the reactants, as the total numbers of π-bonds are higher. To be able to recover the correlation energy in a system requires high angular momentum functions. B3LYP and, especially MP2, needs these high angular momentum functions to properly describe the correlation energy.[22] This improved description of correlation energy of the reactants will result in less exothermic reaction energies with larger basis sets. The MP2 single point energies also show the same basis set trend but to a lesser degree except when the aug-cc-pVTZ basis set is used. When diffuse functions are included, the reaction energy becomes more exothermic by 2 kJ/mol compared to the cc-pVTZ basis set. It should be noted that the MP2 values are much less sensitive to basis set effects than are B3LYP values.

The reactions we have studied here are all proceeding by a concerted one-step formation of products. The reactions might, however, also proceed by a two-step reaction where the first

step consists of a protonation of the alkene, which thus forms a C−O bond to the cluster (alkoxy-group formation). The second step then consists of a breaking of the C−O bond and formation of a C−C bond between the alkyl group and the arene. The carbocation thus formed will, essentially simultaneously, transfer the proton in ipso-position to the alkyl group on the arene back to the cluster. We have not explored these reactions. Preliminary data suggest that the second step of the two-step mechanism implies a much higher activation barrier than the concerted mechanism. The large barrier appears to be caused by the high exothermicity of alkoxide formation. The issue ments further study. A more in-depth discussion is given by Svelle et al. in a paper where the very similar reaction system, dimerization of alkenes, is studied.[28]

4.2. Methanol-to-Hydrocarbons Reaction. The elimination of an alkene, like ethene or propene, from an ethyl/propylarene is thought to be an important step in the MTH mechanism. In the "hydrocarbon-pool" mechanism of methanol conversion on acidic zeolites, the pool splits off a product molecule, an alkene. From experimental data, it is clear that higher methylated benzenes are more reactive in the MTH reaction than lower methylated benzenes.[13,14] Sassi et al.[18] concluded that ethene and propene are more readily eliminated from ethylbenzene and cumene in the presence of methanol, with a possible explanation being that the methanol further methylates the arenes, thereby facilitating alkene elimination. Two schemes for transformations leading to methyl groups being transferred to longer alkyl side chains have been proposed in the litterature: The paring mechanism[30] and side-chain alkylation.[18,31] The initial stages in the reaction leading to the alkyl group breaking away from the arene are not known, but in the final stages the reaction must pass the transition states (in the inverse direction) that have been found here.

In the present work we are able to consider alkene elimination from a neutral ethyl/propyl arene. The neutral ethyl/propylarene is supposed to be protonated first. If the proton becomes bonded to the carbon that is binding the ethyl/propyl group, alkene elimination is facilitated. Protonated arenes are, however, not found to exist as stable "free" charged species in a zeolite.[27] In an earlier work,[15] we showed that in the case of protonated methylbenzenes coadsorbed with water there may be a potential energy surface minimum on a cluster model, such as the one used in this work. Without water present, it was not possible to locate a minimum with protonated methylbenzenes without forming an alkoxy bond between the arene and the zeolite model. In the present work, there is no water, and protonated species are probably transient. A transient protonated species might, however, exist long enough to undergo reactions such as, e.g., isomerizations, dealkylation, or transalkylation. The exact mechanism whereby alkene formation takes place is not considered here.

Transition states found on cluster models have been confirmed to be very similar to those transition states found by calculations on periodic models.[26,27] It may therefore be valid to consider the elimination of ethene and propene in light of the work done by Rozanska et al.[27] on isomerization and disproportionation reactions. The alkene elimination might start with the alkylarene to be (initially) protonated and then reorient itself while staying protonated until it undergoes an alkene elimination by passing the transition state in the reverse direction of the of the arene alkylation studied above.

With an increasing number of methyl groups on the aromatic ring, the transition state energies become lower, and the reaction energies become less exothermic. Hence, by the principle of microscopic reversibility, the barrier height for the reverse reaction, splitting off the alkene from a neutral alkylarene, is also lowered by increasing the number of methyl groups on the arene.

5. Conclusions

We have demonstrated that the direct arene alkylation by ethene and propene proceeds through similar transition states. The zeolite proton attacks the double bond at the same time as a C−C bond is formed between the alkene and the arene. In the transition state, the alkene is not yet fully protonated. In the case of isopropylation the proton transfer is, however, further advanced than in the cases of ethylation or *n*-propylation. The activation energies for *n*-propylation exceed those of ethylation, and isopropylation. The difference between benzene *n*-propylation and isopropylation activation energies is large enough to explain the amount of *n*-propylbenzene formation in cumene production.

The calculated transition state energies agree with the reported effect that presence of methanol facilitates elimination of alkyl groups from alkylbenzenes. Transition state energies for splitting off ethene and propene become lower by introducing methyl groups on the aromatic ring.

The energy trends appear to be rather insensitive to the choice of method, and the B3LYP/6-31G* scheme appears to be sufficient for studies of energy trends in systems such as the ones studied.

Acknowledgment. Thanks are due to the Norwegian Research Council for financial support through grants 135867/431 and 149326/431, and a grant of computer time through the NOTUR project (accounts No. NN2147K and NN2878K).

Supporting Information Available: *XYZ* coordinates for all stationary states, and figures showing the 12 transition states discussed in the text. Figures with arrows showing the normal mode for the transition states for the ethylation, *n*-propylation, and isopropylation of benzene and isopropylation of toluene are also included. This material is available free of charge via the Internet at http://pubs.acs.org.

References and Notes

(1) Degnan, T. F.; Smith, C. M.; Venkat, C. R. *Appl. Catal. A* **2001**, *221*, 283−294.
(2) Cejka, J.; Wichterlova, B.; Bedarova, S. *Appl. Catal. A* **1991**, *79*, 215−226.
(3) Engelhardt, J.; Kallo, D.; Zsinka, I. *J. Catal*. **1992**, *135*, 321−324.
(4) Villarreal, N. E.; Kharisov, B. I.; Ivanova, I. I.; Romanskii, B. V. *Appl. Catal. A* **2002**, *224*, 161−166.
(5) Parikh, P. A.; Subrahmanyam, N.; Bhat, Y. S.; Halgeri, A. B. *Appl. Catal. A* **1992**, *90*, 1−10.
(6) Fraenkel, D.; Levy, M. *J. Catal.* **1989**, *118*, 10−21.
(7) Cejka, J.; Kapustin, G. A.; Wichterlova, B. *Appl. Catal. A* **1994**, *108*, 187−204.
(8) Cejka, J.; Wichterlova, B. *Catal. Rev*. **2002**, *44*, 375−421.
(9) Dahl, I. M.; Kolboe, S. *Catal. Lett*. **1993**, *20*, 329−336.
(10) Dahl, I. M.; Kolboe, S. *J. Catal*. **1994**, *149*, 458−464.
(11) Dahl, I. M.; Kolboe, S. *J. Catal*. **1996**, *161*, 304−309.
(12) Mikkelsen, Ø.; Rønning, P. O.; Kolboe, S. *Microporous Mesoporous Mater.* **2000**, *40*, 95−113.
(13) Arstad, B.; Kolboe, S. *Catal. Lett*. **2001**, *71*, 209−212.
(14) Arstad, B.; Kolboe, S. *J. Am. Chem. Soc*. **2001**, *123*, 8137−8138.
(15) Arstad, B.; Kolboe, S.; Swang, O. *J. Phys. Chem. B* **2002**, *106*, 12722−12726.
(16) Song, W.; Fu, H.; Haw, J. F. *J. Am. Chem. Soc*. **2001**, *123*, 4749−4754.
(17) Song, W.; Haw, J. F.; Nicholas, J. B.; Heneghan, C. S. *J. Am. Chem. Soc*. **2000**, *122*, 10726−10727.

(18) Sassi, A.; Wildman, M.; Ahn, H. J.; Prasad, P.; Nicholas, J. B.; Haw, J. F. *J. Phys. Chem. B* **2002**, *106*, 2294−2303.
(19) Vos, A. M.; Schoonheydt, R. A.; De Proft, F.; Geerlings, P. *J. Phys. Chem. B* **2003**, *107*, 2001−2008.
(20) Frisch, M. J.; Trucks, G. W.; Schlegel, H. B.; Scuseria, M. A.; Robb, M. A.; Cheeseman, J. R.; Zakrzewski, V. G.; Montgomery, J. A.; Stratmann, R. E.; Burant, J. C.; Dapprich, S.; Millam, J. M.; Daniels, A. D.; Kudin, K. N.; Strain, M. C.; Farkas, O.; Tomasi, J.; Barone, V.; Cossi, M.; Cammi, R.; Mennucci, B.; Pomelli, C.; Adamo, C.; Clifford, S.; Ochterski, J.; Petersson, G. A.; Ayala, P. Y.; Cui, Q.; Morokuma, K.; Malick, D. K.; Rabuck, D. K.; Raghavachari, K.; Foresman, J. B.; Cioslowski, J.; Ortiz, J. V.; Stefanov, B. B.; Liu, G.; Liashenko, A.; Piskorz, P.; Komaromi, I.; Gomperts, R.; Martin, R. L.; Fox, D. J.; Keith, T.; Al-Laham, M. A.; Peng, C. Y.; Nanayakkara, A.; Gonzales, C.; Challacombe, M.; Gill, P. M. W.; Johnson, B. G.; Chen, W.; Wong, M. W.; Andres, J. L.; Head-Gordon, M.; Replogle, E. S.; Pople, J. A. *Gaussian 98*, revision A.11.; Gaussian, Inc.: Pittsburgh, PA, 1998.
(21) Corma, A.; Martinez-Soria, V.; Schnoeveld, E. *J. Catal*. **2000**, *192*, 163−173.
(22) Koch, W.; Holthausen, M. C. *A Chemist's Guide to Density Functional Theory*; Wiley: New York, 2000; ISBN 3-527-29918-1.
(23) Wichterlova, B.; Cejka, J. *J. Catal*. **1994**, *146*, 523−529.
(24) Sponer, J.; Sponer, J.; Cejka, J.; Wichterlova, B. *J. Phys. Chem. B* **1998**, *102*, 7169−7175.
(25) Svelle S.; Arstad, B.; Kolboe, S.; Swang, O. *J. Phys. Chem. B* **2003**, *107*, 9281−9289.
(26) Vos, A. M.; Rozanska, X.; Schoonheydt, R. A.; van Santen, R. A.; Hutschka, F.; Hafner, J. *J. Am. Chem. Soc*. **2001**, *123*, 2799−2809.
(27) Rozanska, X.; Van Santen, R. A.; Hutschka, F.; Hafner, J. *J. Am. Chem. Soc*. **2001**, *123*, 7655−7667.
(28) Svelle S.; Kolboe, S.; Swang, O. *J. Phys. Chem. B*, submitted for publication.
(29) Arstad, B.; Nicholas, J. B.; Haw, J. F. *J. Am. Chem. Soc*., in press.
(30) Sullivan, R. F.; Egan, C. J.; Langlois, G. E.; Sieg, R. P. *J. Am. Chem. Soc*. **1961**, *83*, 1156−1160.
(31) Mole, T.; Whiteside, J. A.; Seddon, D. *J. Catal*. **1983**, *82*, 261−266.
(32) NIST Chemistry WebBook (http://webbook.nist.gov/chemistry/).